



Title	Noise sensitivity of physical reservoir computing in a ring array of atomic switches
Author(s)	Kubota, Hiroshi; Hasegawa, Tsuyoshi; Akai-Kasaya, Megumi; Asai, Tetsuya
Citation	Nonlinear theory and its applications, IEICE, 13(2), 373-378 <a href="https://doi.org/10.1587/nolta.13.373">https://doi.org/10.1587/nolta.13.373</a>
Issue Date	2022
Doc URL	<a href="http://hdl.handle.net/2115/85562">http://hdl.handle.net/2115/85562</a>
Rights	Copyright ©2022 The Institute of Electronics, Information and Communication Engineers
Type	article
File Information	13_373.pdf



[Instructions for use](#)

Paper

# Noise sensitivity of physical reservoir computing in a ring array of atomic switches

*Hiroshi Kubota*<sup>1a)</sup>, *Tsuyoshi Hasegawa*<sup>2</sup>,  
*Megumi Akai-Kasaya*<sup>1,3</sup>, and *Tetsuya Asai*<sup>1</sup>

<sup>1</sup> Graduate School of Information Science and Technology, Hokkaido University  
Kita 14, Nishi 9, Sapporo, Hokkaido 060-0814, Japan

<sup>2</sup> School of Advanced Science and Engineering, Waseda University  
3-4-1 Okubo, Shinjuku-ku, Tokyo 169-8555, Japan

<sup>3</sup> Department of Chemistry, Graduate School of Science, Osaka University  
1-1 Machikaneyama, Toyonaka, Osaka 560-0043, Japan

<sup>a)</sup> [kubota.hiroshi.ik@ist.hokudai.ac.jp](mailto:kubota.hiroshi.ik@ist.hokudai.ac.jp)

Received October 18, 2021; Revised December 17, 2021; Published April 1, 2022

**Abstract:** Reservoir computing (RC) is possible using physical systems. We have previously proposed an RC for ideal atomic switches. When temporal current fluctuations (noise) from the measurement of actual atomic switches are introduced into the proposed RC, performance degrades significantly. To address this issue, we propose novel methods for increasing the operating current range and observing the atomic switch several times to determine the average noise. Consequently, the memory capacity of the RC model increased, despite the presence of noise. To improve the precision of RC, we investigated the capacity and showed that changing the time constant of atomic switches results in an improvement.

**Key Words:** atomic switch, neural networks, physical reservoir computing, delayed feedback reservoir computing

## 1. Introduction

Reservoir computing (RC) is a type of recurrent neural network (RNN) architecture that exhibits temporal dynamic behavior [1] and can be implemented in physical systems [2]. Therefore, various physical RCs (PRCs) have been proposed (e.g., optical, spintronics, soft and elastic material, molecular, and field programmable gate array) [3–7]. Our proposed atomic switch PRC exhibits superior power scale, readability, spatial and temporal scalability, and mass producibility [8]. We simulated and evaluated the proposed RC with ideal atomic switches and obtained a large memory capacity (MC) with high precision [9]. In this paper, we introduce a measured current fluctuation from an actual atomic switch (noise) into our RC model, and evaluate the change in performance. Although the MC is decreased, and the error is increased, owing to the noise, we devise a method for improving

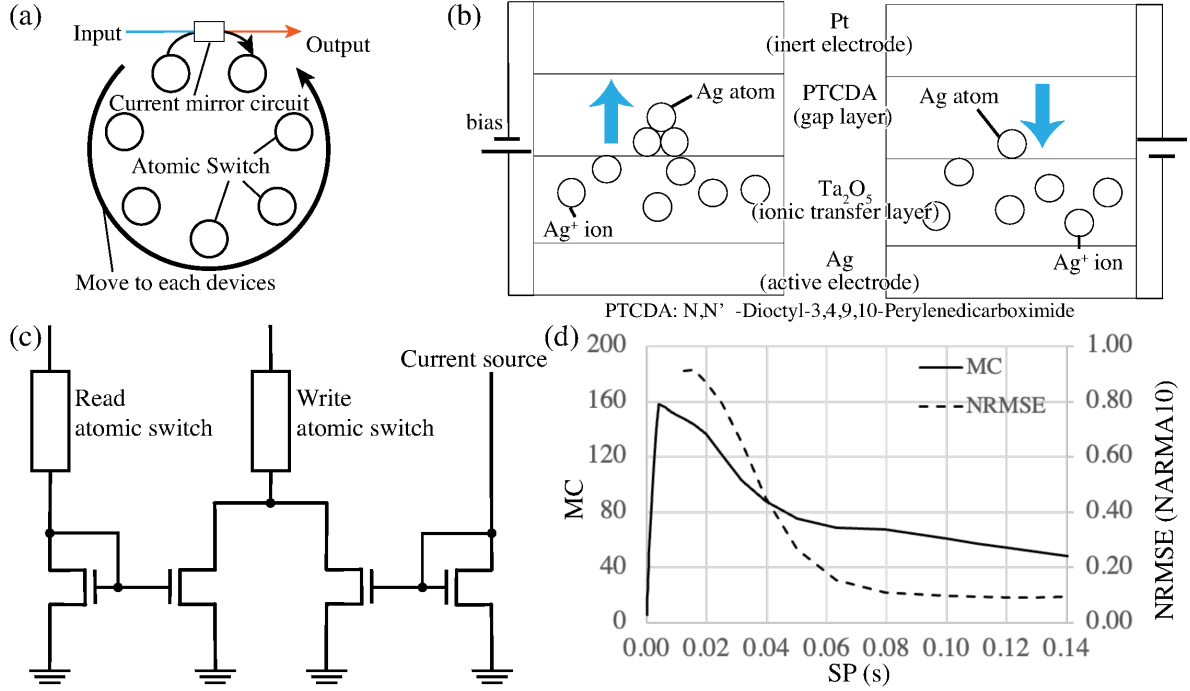


**Fig. 1.** (a) Structure of proposed atomic switch reservoir, (b) structure of the molecular gap atomic switch, (c) current mirror circuit used in our RC used to read and write data (headers), (d) performance of previous atomic switch reservoirs: SP vs. MC & the normalized the root-mean-square error (NRMSE) (NARMA10 task).

the RC performance and confirm it using the simulation.

## 2. Reservoir on atomic switches

The structure of the proposed atomic switch RC is illustrated in Fig. 1 (a). RC on the atomic switches uses the structure of a delayed feedback reservoir (DFR), which uses time-division multiplexing input data for reservoir calculations [10]. In a conventional DFR, the time-multiplexed input value is written into a delayed-loop structure through the nonlinear calculation module. In our proposed DFR, the input data are recorded in the devices, and the input/output current mirror circuit (header) (Fig. 1 (c)) is moved, and it can represent the same structure as conventional DFR.

We used molecular-gap atomic switches (Fig. 1 (b)) as the memory devices [11]. In an atomic switch, the atoms form a filament between the electrodes, which controls the bias input, and it changes the resistance exponentially. When a positive bias is applied, the atoms are deposited, and the resistance decreases. When a negative bias or no bias is applied, the atoms are ionized and dissolved, and the resistance increases. Because the atomic switch has superior characteristics for reservoir calculation, such as nonlinearity and short-term memory, the atomic switch RC is expected to provide high performance. When the device is applied with a bias greater than the threshold bias for a certain time, it maintains a lower resistance (ON state). However, in our PRC, the device does not switch, and we use it with a small bias because an excessively large resistance change is not appropriate for use in RC calculation (OFF state).

Figure 1 (d) shows the simulation result of this reservoir with 201 RC nodes [9]. We obtained large MCs and low NRMSE with the NARMA10 task, finding that the RC performance was affected by the scan period, which is the during of the header moving of the reservoir loop.

## 3. Measurement of the atomic switch

We measured the atomic switches to introduce current fluctuations from the actual device to our RC model. The structure of the measured atomic switch (Fig. 2 (a)) is Pt (30 nm), N,N' - diheptylperylene-tetracarboxylic diimide (PTCDI) (6 nm), Ta<sub>2</sub>O<sub>5</sub> (2 nm), mixed layer of Ta<sub>2</sub>O<sub>5</sub> and

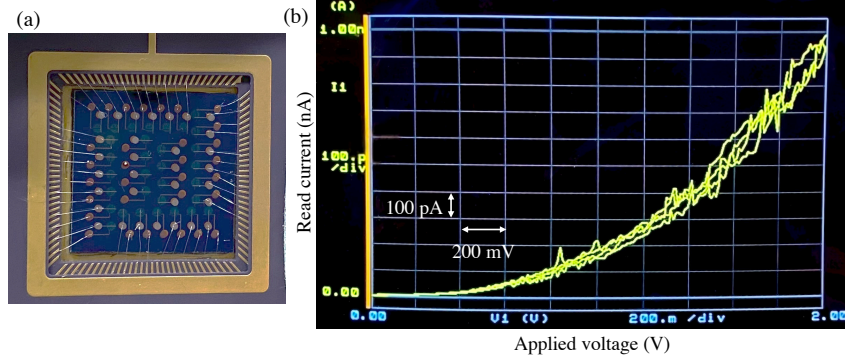


**Fig. 2.** (a) Atomic switches, (b) I-V curve of atomic switch for measuring in “short” and “append” with an Agilent 4156c precision semiconductor parameter analyzer.

Cu (22 nm), Cu (10 nm), Pt (10 nm), and Au (50 nm) from the top. The Pt layer is the top electrode, the PTCDI layer is the molecular gap, the Ta<sub>2</sub>O<sub>5</sub> layer and the mixed layer of Ta<sub>2</sub>O<sub>5</sub> and Cu are the ionic transfer layer, the Cu layer is the ion resource, and the Pt and Au layers are the bottom electrode. Figure 2 (b) shows that the results of I-V measurements five times in “short” and “append” of the atomic switch using an Agilent 4156c precision semiconductor parameter analyzer. As can be seen, current fluctuations occur when a voltage is applied to the atomic switch. The current fluctuation (noise) was introduced into the atomic switch model.

#### 4. Introduction of noise model

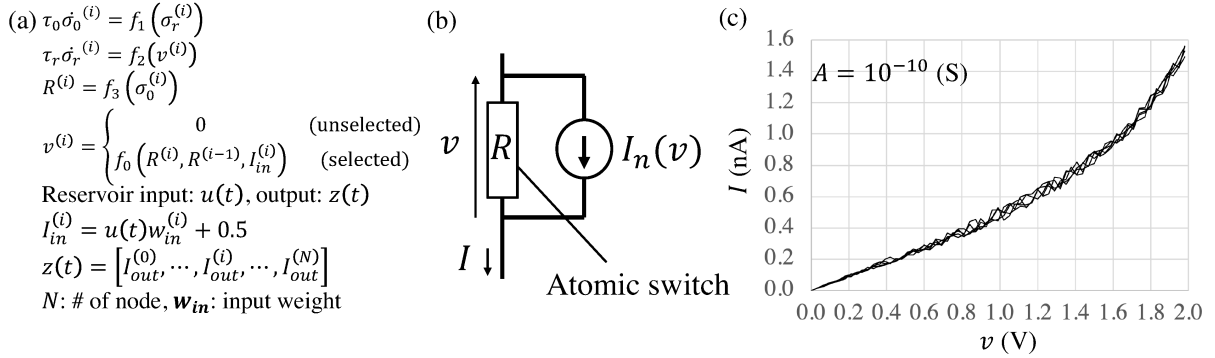


**Fig. 3.** (a) Reservoir model [9], (a) noise model, (b) I-V Curve of atomic switch with noise model in simulation.

To introduce noise into model, we propose the current source shown in Fig. 3 (b) and simulated it using the proposed atomic switch models [9], which are

$$\tau_r \dot{\sigma}_r = -(\sigma_r - \alpha v), \quad \tau_0 \dot{\sigma}_0 = -(\sigma_0^3 - (\sigma_0 - V_d) - \sigma_r), \quad (1)$$

$$R = k_R \exp\{-\beta \times f(\sigma_0)\}, \quad f(\sigma_0) = \tanh(s \times (\sigma_0 - d)) - g \times (\sigma_0 - 1), \quad (2)$$

where  $v$  is the applied bias;  $R$  is the device resistance in Fig. 3 (b);  $\sigma_r$  and  $\sigma_0$  are variables;  $\alpha$ ,  $\beta$ ,  $V_d$ ,  $s$ ,  $g$ , and  $d$  are constants; and  $\tau_r$  and  $\tau_0$  are time constants. Then, the RC equations are written as shown in Fig. 3 (a). Figure 2 (c) shows that the noise increases in proportion to the voltage in the small voltage range, but it does not increase when the voltage is large. In our model, the value of the current source is increased in proportion to the voltage in  $v < 1$ , where  $v$  is the voltage applied to the atomic switch and the constant value of the noise range in  $v \geq 1$ . The value of the current source  $I_n(v)$  in Fig. 3 (b) is

$$I_n(v) = \begin{cases} A \cdot n(t) \cdot v & (v < 1) \\ A \cdot n(t) & (v \geq 1) \end{cases}, \quad (3)$$

where  $A$  is the amplitude of the noise, and  $n(t)$  is a uniform random number ( $0 \leq n(t) \leq 1$ ).

Figure 3 (c) shows the results of simulation the I–V characteristics of the model with the current source shown in Fig. 2 (b). The voltage was swept from 0 to 2 V, and the current was measured four times. The noise amplitude of  $I_n(v)$  was set to  $A = 10^{-10}$  to match the measurement results of the actual atomic switch. The result was similar to that of Fig. 2 (c).

## 5. Simulation Results

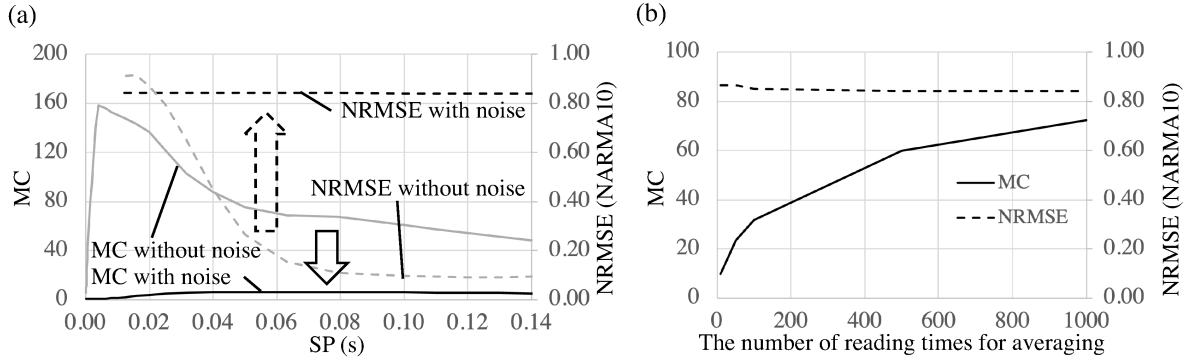


**Fig. 4.** (a) SP vs. MC & NRMSE (NARMA10 task) about RC model with and without noise, (b) the number of average vs. MC & NRMSE (NARMA10 task).

Figure 4 (a) shows the simulation results of atomic switch RC with noise model. In this RC, the MC and NRMSE deteriorated significantly. Therefore, we considered two methods to improve the performance of this PRC.

### 5.1 Current range increase

The first method proceeds as follows. In previous simulations, the input/output current mirrors were operated at a sub-threshold current. It was made to operate at an over-threshold to improve the signal-to-noise ratio. First, we increase the input from the current mirror circuit (the value of the “current source” in Fig. 1 (c)) from  $\sim 1$  nA to  $\sim 100$  nA. However, when the input is increased, the voltage between the two ends of the atomic switch on the write side is fixed to the power-supply voltage (the voltage at the lower end of the atomic switch becomes zero), owing to the high resistance of the atomic switch. Therefore, the input value of RC is not fully reflected in the atomic switch. To solve this problem, we must increase the supply voltage and/or reduce the resistance of the atomic switch. Hence, we set the supply voltage to 3 V. Additionally, because the resistance of the atomic switch in the OFF state can be changed, the simulation of this RC was conducted with the OFF resistance of the atomic switch set to one-tenth of the value of the previous RC.

### 5.2 Average the reading data

Second, we considered taking multiple readings of the atomic switches and averaging the readings to reduce the effect of noise. Figure 4 (b) shows the relationship between the average number of times and MC and NRMSE of the NARMA10 task (SP = 0.02 s in MC, SP = 0.13 s in NRMSE of the NARMA10 task) of atomic switch RC after increasing current range. Increasing the average number of readings improved the MC, but the NRMSE did not improve.

## 6. Nonlinearity of the atomic switches in the RC

Because the NRMSE of the NARMA10 task did not improve, we measured the capacity to determine the cause of the problem. The capacity can help evaluate the short-term memory capacity for higher-order target signals. Here, the capacity is the sum of the squared correlation coefficients of prediction for the delayed polynomial equation, which is a Legendre polynomial, consists for a certain degree, and proposed in [12]. The capacity of the proposed RC is illustrated in Fig. 5 (b). In this figure,

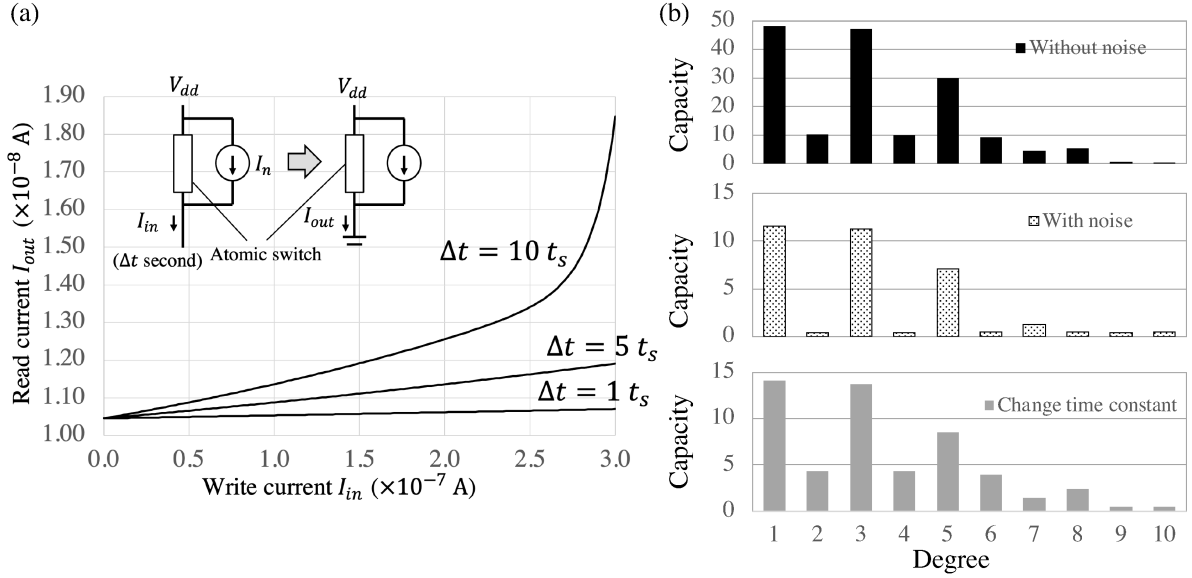


**Fig. 5.** (a) Input/output characteristics of atomic switch dependence input duration, (b) capacity of atomic switch RC without noise, with noise, and after change the attenuation time constant.

the horizontal axis represents the order of the target function, and the vertical axis represents the capacity. Comparing the capacity with and without noise, we found that the capacity of some orders is missing. To explore the cause, we investigated the input–output characteristics of the atomic switch model before the introduction of noise. Figure 5 (a) shows the result of reading the current value after input from the current source for  $\Delta t$  s and waiting for  $t_w$  s. It is shown that  $\Delta t = t_s$ ,  $5t_s$ , and  $10t_s$ , where  $t_s$  is the duration of the input node when the NRMSE is the lowest in the RC model, which is represented as  $t_s = SP/N$ , where  $N$  is the number of RC nodes, and  $SP = 0.13$  s. The waiting duration of  $t_w$  is the duration between the input to the atomic switch and the next readout in the RC model, which is represented by  $t_w = SP/N \times (N - 1)$ .

Figure 5 (a) shows that the nonlinearity of the atomic switch could not be utilized when inputting the data with  $\Delta t$ , which is used in our RC. When  $\Delta t$  is increased ( $\Delta t = 10t_s$ ), the RC calculation can be performed within the range where the nonlinear region of the atomic switch can be utilized. However, when  $t_s$  is increased, the data attenuation in the RC is excessive, and the RC performance cannot be improved.

To prevent excessive attenuation in the RC, even when  $t_s$  is increased, we considered an atomic switch having a long attenuation time constant ( $\tau_a$ ), which is a parameter that determines the rate of resistance change when the voltage is stopped compared with the input time constant ( $\tau_b$ ), which is a parameter that determines the rate of resistance change when the voltage is applied. In our atomic switch model, the input time constant and the attenuation time constant are the same, but some actual devices behave in such a way that they are different. Additionally, when the attenuation time constant was increased, it became possible to use the nonlinear region of the atomic switch without changing  $t_s$ , because there is an offset at the next input of one input. The capacity when  $\tau_a = 16\tau_b$  is shown in Fig. 5 (b). The order capacity, which was missing for the RC with noise, was recovered.

## 7. Conclusions

The RC was simulated with a model that introduced current fluctuations measured in an atomic switch into our design, and the performance deteriorated. To improve the RC performance, the range of the input current of the current mirror was increased, and the current readout of the atomic switch was averaged repeatedly. As a result, the MC improved, but the NRMSE of the NARMA10 task did not improve. The capacity was investigated, and it was shown that capacities of some order were missing. To solve this problem, we considered taking advantage of the nonlinearity of the atomic

switch. As a result of simulating with a model in which the time constant at attenuation was longer than the time constant at input, we found that we can utilize the nonlinearity, and the capacity is improved.

## Acknowledgments

This work is partly based on the results obtained from a project (JPNP16007) subsidized by the New Energy and Industrial Technology Development Organization (NEDO).

## References

- [1] H. Jaeger, “The “echo state” approach to analysing and training recurrent neural networks,” *Technical Report GMD*, Report 148, German National Research Center for Information Technology, 2001.
- [2] M. Lukoševičius and H. Jaeger, “Reservoir computing approaches to recurrent neural network training,” *Computer Science Review*, vol. 3, no. 3, pp. 127–149, August 2009. DOI: 10.1016/j.cosrev.2009.03.005
- [3] G. Van der Sande, D. Brunner, and M. Soriano, “Advances in photonic reservoir computing,” *Nanophotonics*, vol. 6, no. 3, pp. 561–576, May 2017. DOI: 10.1515/nanoph-2016-0132
- [4] R. Nakane, G. Tanaka, and A. Hirose, “Reservoir computing with spin waves excited in a garnet film,” *IEEE Access*, vol. 6, pp. 4462–4469, January 2018. DOI: 10.1109/ACCESS.2018.2794584
- [5] K. Nakajima, H. Hauser, R. Kang, E. Guglielmino, D. G. Caldwell, and R. Pfeifer, “Computing with a muscular-hydrostat system,” *2013 IEEE International Conference on Robotics and Automation*, pp. 1504–1511, May 2013. DOI: 10.1109/ICRA.2013.6630770
- [6] H. Tanaka, M. Akai-Kasaya, A. TermehYousefi, L. Hong, L. Fu, H. Tamukoh, D. Tanaka, T. Asai, and T. Ogawa, “A molecular neuromorphic network device consisting of single-walled carbon nanotubes complexed with polyoxometalate,” *Nature Communications*, vol. 9, no. 1 p. 2693, July 2018. DOI: 10.1038/s41467-018-04886-2
- [7] M. L. Alomar, M. C. Soriano, M. Escalona-Morán, V. Canals, I. Fischer, C. R. Mirasso, and J. L. Rosselló, “Digital implementation of a single dynamical node reservoir computer,” *IEEE Transactions on Circuits and Systems II: Express Briefs*, vol. 62, no. 10, pp. 977–981, October 2015. DOI: 10.1109/TCSII.2015.2458071.
- [8] T. Hasegawa, K. Terabe, T. Tsuruoka, and M. Aono, “Atomic switch: atom/ion movement controlled devices for beyond von-Neumann computers,” *Advanced Materials*, vol. 24, no. 2, pp. 252–267, January 2012. DOI: 10.1002/adma.201102597
- [9] H. Kubota, T. Hasegawa, M. Akai-Kasaya, and T. Asai, “Reservoir computing on atomic switch arrays with high precision and excellent memory characteristics,” *Journal of Signal Processing*, vol. 25, no. 4, pp. 123 – 126, July 2021. DOI: 10.2299/jsp.25.123
- [10] L. Appeltant, M.C. Soriano, G. Van der Sande, J. Danckaert, S. Massar, J. Dambre, B. Schrauwen, C.R. Mirasso, and I. Fischer, “Information processing using a single dynamical node as complex system,” *Nature Communications*, vol. 2, no. 1, p. 468, September 2011. DOI: 10.1038/ncomms1476
- [11] A. Suzuki, T. Tsuruoka, and T. Hasegawa, “Time-dependent operations in molecular gap atomic switches,” *Physica Status Solidi B*, vol. 256, no. 8, p. 1900068, April 2019. DOI: 10.1002/pssb.201900068
- [12] S. Kan, K. Nakajima, Y. Takeshima, T. Asai, Y. Kuwahara, and M. Akai-Kasaya, “Simple reservoir computing capitalizing on the nonlinear response of materials: Theory and Physical Implementations,” *Physical Review Applied*, vol. 15, no. 2, p. 024030, February 2021. DOI: 10.1103/PhysRevApplied.15.024030